Compositional Modeling With an Equation of State

L.X. Nghiem, SPE, Computer Modelling Group
D.K. Fong,* SPE, Computer Modelling Group
K. Aziz, SPE, Computer Modelling Group

Abstract

This paper describes an implicit-pressure explicit-composition and explicit-saturation compositional model. The model uses an equation of state (Peng-Robinson) for phase equilibrium and density calculations. Interfacial tension effects are considered also. The formulation of the pressure equation yields a symmetric and diagonally dominant matrix that allows the use of the iterative conjugate gradient method for large systems. Simulation of laboratory CO_2 displacements shows good agreement between calculated and experimental results. The influence of interfacial tension is investigated. Physically reasonable results also have been obtained for hypothetical areal and cross-sectional problems.

Introduction

The design of high-pressure-gas, enriched-gas, or CO_2-injection schemes requires an accurate prediction of the vapor-liquid equilibrium between the oil-in-place and the injected fluid. In recent years, vapor-liquid equilibrium calculations have been enhanced by the introduction of many two-constant equations of state that can be applied to both the vapor and liquid phases.[1-3] The application of these equations of state to petroleum reservoir fluids was made possible by the ability to evaluate the parameters of these equations from properties of the heavy fraction—i.e., density, average boiling point, and molecular weight[4-6]—which can be measured easily.

Two compositional models that utilize an equation of state for phase equilibrium and properties calculation are described by Fussell and Fussell[7,8] and Coats.[9] When both gas and oil are present in every grid block, the formulation of Fussell and Fussell requires the simultaneous solution of $n_b(\nu + 1)$ nonlinear equations, where n_b is the number of grid blocks and ν is the number of components in the hydrocarbon system. The explicit treatment of the transmissibilities limits the size of the allowable time step. On the other hand, Coats proposed a fully implicit equation-of-state compositional model. His formulation requires the simultaneous solution of $n_b(2\nu + 4)$ equations. Although the stability of Coats' model is better than that of Fussell and Fussell's model, the computational cost of Coats' implicit model may become prohibitive for systems containing a large number of grid blocks and components.

This paper presents an implicit-pressure, explicit-composition and saturation equation-of-state compositional model that is a variation of that proposed by Kazemi *et al.*[10] The formulation of the pressure equation yields a symmetric and diagonally dominant matrix that allows the use of the iterative conjugate gradient method for large systems. The diagonal dominance is also a desirable feature for the numerical stability of direct elimination methods.

An efficient method for flash calculation[11] allows the use of the model in the vicinity of the critical point and avoids the computation of the saturation pressure in determining the single-phase region.

A new model for relative permeabilities that is dependent on interfacial tension is proposed and the sensitivity of the recovery to interfacial tension is discussed.

A well model that allows the simulation of constant volume, constant injection/production wells and multiblock well completions is provided.

The Peng-Robinson equation of state[3] is used in all examples, although the solution method is general and applicable for any other equation of state.

Mathematical Model

Flow Equations

Assuming Darcy's law is valid, the material balance on

*Now with Shell Canada Resources Ltd.

0197-7520/81/0012-9306$00.25

the water phase and ν hydrocarbon components yields the following $\nu + 1$ difference equations.

$$\Delta T_w^n \left(\Delta p_o^{n+1} - \Delta P_{cwo}^n - \gamma_w^n \Delta D\right) = \frac{V_b}{\Delta t}\left[\left(\phi \rho_w S_w\right)^{n+1} - \left(\phi \rho_w S_w\right)^n\right] \quad \ldots\ldots (1)$$

and

$$\Delta\left[T_o^n y_{mo}^n \left(\Delta p_o^{n+1} - \gamma_o^n \Delta D\right) + T_g^n y_{mg}^n \cdot \left(\Delta p_o^{n+1} + \Delta P_{cog}^n - \gamma_g^n \Delta D\right)\right] + q_m = \frac{V_b}{\Delta t}\left[\phi^{n+1}\left(\rho_o S_o + \rho_g S_g\right)^{n+1} z_m^{n+1} - \phi^n \left(\rho_o S_o + \rho_g S_g\right) z_m^n\right],$$

$$m = 1 \ldots \nu. \quad \ldots\ldots (2)$$

The molar balance equation of the hydrocarbon system is obtained by summing Eq. 2 over ν hydrocarbon components:

$$\Delta\left[T_o^n \left(\Delta p_o^{n+1} - \gamma_o^n \Delta D\right) + T_g^n \left(\Delta p_o^{n+1} + \Delta P_{cog}^n - \gamma_g^n \Delta D\right)\right] + q_h = \frac{V_b}{\Delta t}\left[\phi^{n+1}\left(\rho_o S_o + \rho_g S_g\right)^{n+1} - \phi^n \left(\rho_o S_o + \rho_g S_g\right)^n\right], \quad \ldots\ldots (3)$$

where

$$q_h = \sum_m q_m. \quad \ldots\ldots (4)$$

Equilibrium Equations

It is assumed that interphase thermodynamic exchange in the reservoir is rapid compared with fluid flow so that the gas and oil are in phase equilibrium. It also is assumed that mass transfer between the water and hydrocarbon phases is negligible.

The thermodynamic equilibrium conditions are given by the equality of the component fugacities in the oil and gas phases—i.e.,

$$f_{mo} = f_{mg}, \quad m = 1 \ldots \nu. \quad \ldots\ldots (5)$$

From a material balance on the oil and gas phases, the following algebraic equations are obtained.

$$z_m = L y_{mo} + V y_{mg}, \quad m = 1 \ldots \nu, \quad \ldots\ldots (6)$$

$$L = \frac{\rho_o S_o}{\rho_o S_o + \rho_g S_g}, \quad \ldots\ldots (7)$$

and

$$V = \frac{\rho_g S_g}{\rho_o S_o + \rho_g S_g}, \quad \ldots\ldots (8)$$

The fugacities, f_{mo} and f_{mg}, and molar densities, ρ_o and ρ_g, are computed at pressure p_o.

Constraint Equations

The definition of mole fractions and saturations gives the additional constraint equations:

$$\sum_m z_m = \sum_m y_{mo} = \sum_m y_{mg} = 1, \quad \ldots\ldots (9)$$

$$L + V = 1, \quad \ldots\ldots (10)$$

and

$$S_o + S_g + S_w = 1. \quad \ldots\ldots (11)$$

Each grid block will have its own set of algebraic equations (Eqs. 5 through 11). The coupling of the variables between adjacent grid blocks is through the Flow Eqs. 1 and 2.

Solution Method

Outline

Eqs. 1 and 2 and 5 through 11 represent a system of $n_b(3\nu + 6)$ equations in $n_b(3\nu + 6)$ unknowns ($p_{o,i}$, $z_{m,i}$, $y_{mo,i}$, $y_{mg,i}$, L_i, V_i, $S_{w,i}$, $S_{o,i}$, and $S_{g,i}$; $i = 1 \ldots n_b$, $m = 1 \ldots \nu$), where n_b and ν are the number of grid blocks and the number of components in the oil/gas system, respectively.

The equations are solved using an iterative-sequential method. Eqs. 1 and 4 are combined to form the pressure equation, which is linearized and solved with either a direct or iterative method. Once $p_o^{(\ell+1)}$, the $(\ell+1)$th iterate of p_o^{n+1}, is obtained, Eq. 1 is solved for $S_w^{(\ell+1)}$ and Eq. 2 is solved for $z_m^{(\ell+1)}$. Flash calculations then are performed to obtain $y_{mo}^{(\ell+1)}$, $y_{mg}^{(\ell+1)}$, $V^{(\ell+1)}$, $L^{(\ell+1)}$, $\rho_o^{(\ell+1)}$, and $\rho_g^{(\ell+1)}$. Finally, Eq. 7 or 8 and Eq. 11 are used to obtain $S_o^{(\ell+1)}$ and $S_g^{(\ell+1)}$. The procedure is repeated until convergence is achieved.

Pressure Equation

The pressure equation is obtained by multiplying Eq. 1 by a constant parameter θ and adding the product to Eq. 4:

$$\Delta\left[\theta T_w^n \left(\Delta p_o^{n+1} - \Delta P_{cwo}^n - \gamma_w^n \Delta D\right) + T_o^n \left(\Delta p_o^{n+1} - \gamma_o^n \Delta D\right) + T_g^n \left(\Delta p_o^{n+1} + \Delta P_{cog}^n - \gamma_g^n \Delta D\right)\right] + \theta q_w + q_h - \frac{V_b}{\Delta t}\left(\phi^{n+1}\alpha^{n+1} - \phi^n \alpha^n\right) = 0, \quad \ldots\ldots (12)$$

where

$$\alpha = \theta \rho_w S_w + \rho_o S_o + \rho_g S_g. \quad \ldots\ldots (13)$$

Since the units of Eq. 1 are moles of H_2O per time and those of Eq. 2 are moles of hydrocarbon per time, it is important to scale these equations appropriately before adding them together. Better convergence can be achieved by introducing the scaling factor, θ, which converts moles of H_2O into equivalent moles of hydrocarbon.

In the program, θ is evaluated at time zero and at a grid block specified by the user using the following equation.

$$\theta = \left.\frac{\rho_o S_o + \rho_g S_g}{\rho_w (S_o + S_g)}\right|_{t=0}. \quad \ldots\ldots\ldots\ldots\ldots\ldots (14)$$

Typical values for molar densities in reservoir engineering problems are: $\rho_o = 6 \times 10^3$ g mol/m^3, $\rho_g = 12 \times 10^3$ g mol/m^3, $\rho_w = 55.6 \times 10^3$ g mol/m^3. Using Eq. 14, θ usually falls in the interval (0.1, 0.2). For practical purposes, any value of θ in that range can be used instead of computing it from Eq. 14.

Pressure Equation Solution

Let F_i denote the left side of Eq. 12 for the ith grid block and let $p_{o,i}^{(\ell+1)}$ be the ℓth iterate of $p_{o,i}^{n+1}$. The $(\ell+1)$th iterate can be obtained from the following Newton-like iteration.

$$\sum_k J_{ik}^{(\ell)} \left[p_{o,k}^{(\ell+1)} - p_{o,k}^{(\ell)}\right] = -F_i^{(\ell)},\ i = 1 \ldots n_b, \quad \ldots\ldots\ldots\ldots (15)$$

where J_{ik} is the ikth element of an approximation to the Jacobian described below. The sum in Eq. 15 is over the ith grid block and its adjacent blocks. The J_{ik}'s are computed as follows.

$$J_{ik}^{(\ell)} = \left(\frac{\partial F_i}{\partial p_{o,k}}\right)^{(\ell)} = \left(\theta T_w + T_o + T_g\right)_{(i+k)/2}^{n} \quad \ldots\ldots\ldots\ldots (16a)$$

and

$$J_{ii}^{(\ell)} = \left(\frac{\partial F_i}{\partial p_{o,i}}\right)^{(\ell)} = -\sum_{\substack{k \\ k \neq i}} \left(\theta T_w + T_o + T_g\right)_{(i+k)/2}^{n} + \theta\left(\frac{\partial q_w}{\partial p_o}\right)_i^{(\ell)} + \left(\frac{\partial q_h}{\partial p_o}\right)_i^{(\ell)} - \frac{V_b}{\Delta t}\left(\frac{\partial \phi\alpha}{\partial p_o}\right)_i, \quad \ldots\ldots\ldots\ldots (16b)$$

where the subscript $(i+k)/2$ denotes the interface between grid blocks i and k.

In Eq. 13, ρ_o is a function of p_o and y_{mo}, and ρ_g is a function of p_o and y_{mg}. The actual derivative of α with respect to p_o will involve the terms $\partial S_w/\partial p_o$, $\partial S_o/\partial p_o$, $\partial S_g/\partial p_o$, $\partial y_{mo}/\partial p_o$, and $\partial y_{mg}/\partial p_o$, which are complicated to compute and will yield partial derivative terms in the off-diagonal elements. An approximation to $(\partial\alpha/\partial p_o)_i^{(\ell)}$ is obtained by neglecting these terms—i.e.,

$$\left(\frac{\partial \alpha}{\partial p_o}\right)_i^{(\ell)} = \left(\theta S_w \frac{\partial \rho_w}{\partial p_o} + S_o \frac{\partial \rho_o}{\partial p_o} + S_g \frac{\partial \rho_g}{\partial p_o}\right)_i^{(\ell)}. \quad \ldots\ldots\ldots\ldots (17)$$

In solving nonlinear equations, an exact Jacobian is not required for convergence. In the approximation of the derivative of α, saturations and compositions are assumed constant while all the pressure-dependent terms are differentiated properly. Saturations and compositions are updated explicitly in α and $\partial\alpha/\partial p_o$ after each iteration. The iterative process is intermediate between simple substitutions and Newton's iteration.

The porosity and molar densities of water, oil, and gas are related to p_o by the following equations.

$$\phi = \phi^*\left[1 + c_f\left(p_o - p_f^*\right)\right]. \quad \ldots\ldots\ldots\ldots (18)$$

$$\rho_w = \rho_w^*\left[1 + c_w\left(p_o - p_w^*\right)\right]. \quad \ldots\ldots\ldots\ldots (19)$$

$$\rho_j = \frac{p_o}{Z_j R T},\ j = o,g. \quad \ldots\ldots\ldots\ldots (20)$$

Hence, the derivative of the accumulation term in Eq. 16b is given by

$$\left(\frac{\partial \phi\alpha}{\partial p_o}\right)_i^{(\ell)} = c_f \phi^* \alpha_i^{(\ell)} + \phi_i^{(\ell)}\left(\theta S_w c_w \rho_w^* + S_o \frac{\partial \rho_o}{\partial p_o} + S_g \frac{\partial \rho_g}{\partial p_o}\right)_i^{(\ell)}, \quad \ldots\ldots (21)$$

where

$$\frac{\partial \rho_j}{\partial p_o} = \frac{1}{R T Z_j}\left(1 - \frac{p_o}{Z_j}\frac{\partial Z_j}{\partial p_o}\right),\ j = o,g. \quad \ldots\ldots (22)$$

Since $\partial\rho_j/\partial p_o$ is positive, it follows that $\partial\phi\alpha/\partial p_o$ is also positive. Furthermore, it is shown later that $\partial q_w/\partial p_o$ and $\partial q_h/\partial p_o$ are negative or zero, depending on the type of well. Examination of Eq. 16 shows that the Jacobian is symmetric and strictly diagonally dominant. The formulation of the pressure equation in Ref. 10 does not yield a symmetric matrix nor does it guarantee diagonal dominance.

The pressure equation is solved using either direct elimination or the iterative conjugate gradient method with incomplete Choleski factorization ICCG(0) as proposed by Meijerink and van der Vorst.[12]

Composition Equation

Composition is computed explicitly at every iteration after $p_o^{(\ell+1)}$ has been determined. Let

$$\Delta\Phi_o^{(\ell+1)} = \Delta p_o^{(\ell+1)} - \gamma_o^n \Delta D \quad \ldots\ldots\ldots\ldots (23)$$

and

$$\Delta\Phi_g^{(\ell+1)} = \Delta p_o^{(\ell+1)} + \Delta P_{cog}^n - \gamma_g^n \Delta D. \quad \ldots\ldots\ldots\ldots (24)$$

An explicit composition equation is obtained by rearranging Eq. 2:

$$z_m^{(\ell+1)} = \left\{\Delta\left[T_o^n y_{mo}^n \Delta\Phi_o^{(\ell+1)} + T_g^n y_{mg}^n \Delta\Phi_g^{(\ell+1)}\right] + q_m + \frac{V_b}{\Delta t}\phi^n\left(\rho_o S_o + \rho_g S_g\right)^n z_m^n\right\} \div \left[\frac{V_b}{\Delta t}\phi^{(\ell+1)}\left(\rho_o S_o + \rho_g S_g\right)^{(\ell+1)}\right]. \quad (25)$$

An approximation to the denominator in Eq. 25 is obtained from Eq. 4:

$$\frac{V_b}{\Delta t}\phi^{(\ell+1)}\left(\rho_o S_o + \rho_g S_g\right)^{(\ell+1)}$$

$$= \Delta\left[T_o^n \Delta\Phi_o^{(\ell+1)} + T_g^n \Delta\Phi_g^{(\ell+1)}\right]$$

$$+ q_h + \frac{V_b}{\Delta t}\phi^n\left(\rho_o S_o + \rho_g S_g\right)^n. \quad \ldots\ldots\ldots (26)$$

Composition as computed previously is guaranteed to satisfy

$$\sum_m z_m^{(\ell+1)} = 1.$$

The method is equivalent to solving Eq. 2 for the number of moles of m and Eq. 3 for the total number of moles of hydrocarbon, and obtaining z_m by taking the ratio.

Saturation Equation

Saturations also are computed explicitly at every iteration. From Eq. 1:

$$S_w^{(\ell+1)} = \frac{\Delta T_w^n \Delta\Phi_w^{(\ell+1)} + q_w^n + \frac{V_b}{\Delta t}\phi^n \rho_w^n S_w^n}{\frac{V_b}{\Delta t}\phi^{(\ell+1)}\rho_w^{(\ell+1)}} \quad \ldots\ldots\ldots\ldots\ldots\ldots\ldots\ldots\ldots\ldots (27)$$

Oil and gas saturations for the $(\ell+1)$th iteration are computed by performing a flash calculation on $z_m^{(\ell+1)}$ $m = 1 \ldots \nu$ at $p_o^{(\ell+1)}$ to obtain $y_{mo}^{(\ell+1)}$, $y_{mg}^{(\ell+1)}$, $\rho_o^{(\ell+1)}$, $\rho_g^{(\ell+1)}$, $V^{(\ell+1)}$, and $L^{(\ell+1)}$. If the results of the flash yield a two-phase system, the oil and gas saturations can be computed from Eqs. 7, 8, and 11:

$$S_o^{(\ell+1)} = \left[\frac{(1-S_w)L\rho_g}{L\rho_g + V\rho_o}\right]^{(\ell+1)} \quad \ldots\ldots\ldots\ldots\ldots\ldots (28)$$

and

$$S_g^{(\ell+1)} = 1 - S_o^{(\ell+1)} - S_w^{(\ell+1)}. \quad \ldots\ldots\ldots\ldots\ldots\ldots (29)$$

If a single-phase system is predicted, then, depending on the nature of the phase,

$$S_o^{(\ell+1)}\left[\text{or } S_g^{(\ell+1)}\right] = 1 - S_w^{(\ell+1)} \quad \ldots\ldots\ldots\ldots\ldots\ldots (30)$$

and

$$S_g^{(\ell+1)}\left[\text{or } S_o^{(\ell+1)}\right] = 0. \quad \ldots\ldots\ldots\ldots\ldots\ldots (31)$$

An efficient flash-calculation method described by Nghiem and Aziz[11] is used. It provides convergence in the vicinity of the critical point and avoids the computation of the saturation pressure to determine the single-phase region.

The attribution of the term "oil" or "gas" to a single-phase fluid around the critical point is meaningless. Therefore, it is arbitrarily named either "oil" or "gas" depending on whether the value of V obtained from flash calculations is zero or one.

Flow Coefficients and Capillary Pressures

This section describes the methods used for evaluating the flow coefficients ($T_o y_{mo}$, $T_g y_{mg}$, and T_w) and the capillary pressures.

By definition,

$$T_j = \frac{A}{\Delta\ell}\frac{k\,k_{rj}}{\mu j}\rho_j, \quad j = o,g,w, \quad \ldots\ldots\ldots\ldots\ldots\ldots (32)$$

where A is the area of the grid block perpendicular to the direction of the grid block length, $\Delta\ell$.

A and $\Delta\ell$ are evaluated at the interface between grid blocks and absolute permeability k is evaluated using the harmonic average. Relative permeability k_r, viscosity μ, and density ρ are evaluated at the upstream block.

Under immiscible conditions, gas/oil relative permeability curves usually show considerable curvature and there are residual oil and gas saturations below which the respective phases are immobile. As the injected fluid and the oil-in-place become gradually miscible through multiple contact, the interfacial tension between the oil and gas decreases toward zero. This will make the relative permeability curves approach straight lines without any residual oil and gas saturations.

The following relative permeability model that exhibits the described behavior at low interfacial tension is used. Let $\tilde{k}_{rg}$ and $\tilde{k}_{rog}$ be the relative permeabilities in the oil/gas system measured under immiscible conditions. Relative permeabilities k_{rg} and k_{rog} at interfacial tension σ are computed using the following equations.

$$k_{rg} = \left(1 - e^{-a_g r}\right)\tilde{k}_{rg} + e^{-a_g r}k_{roiw}$$

$$\cdot\left(\frac{S_g}{1-S_{wr}}\right)^{1+b_g r}, \quad \ldots\ldots\ldots\ldots\ldots\ldots (33a)$$

$$k_{rog} = \left(1 - e^{-a_o r}\right)\tilde{k}_{rog} + e^{-a_o r}k_{roiw}$$

$$\cdot\left(\frac{S_o}{1-S_{wr}}\right)^{1+b_o r}, \quad \ldots\ldots\ldots\ldots\ldots\ldots (33b)$$

$$r = \frac{\sigma}{\sigma^*}, \quad \ldots\ldots\ldots\ldots\ldots\ldots\ldots\ldots (34)$$

$$a_g > 0, \quad \ldots\ldots\ldots\ldots\ldots\ldots\ldots\ldots (35a)$$

and

$$a_o > 0, \quad \ldots\ldots\ldots\ldots\ldots\ldots\ldots\ldots (35b)$$

where a_o, a_g, b_o, and b_g are adjustable parameters. σ^* is a specified interfacial tension introduced for convenience to make r, a_g, b_g, a_o, and b_o dimensionless. Common values used for σ^* are in the range of 1 to 5 dyne/cm. Eq. 33 is based on the requirement that the relative permeabilities to oil or gas in the presence of irreducible water saturation are equal.

Note that for values of σ such that $e^{-a_g\sigma} \simeq 0$ and $e^{-a_o\sigma} \simeq 0$, k_{rg}, and k_{rog} are equal to $\tilde{k}_{rg}$, and $\tilde{k}_{rog}$, respectively. As σ decreases toward zero, k_{rg} and k_{rog} approach the respective straight lines $k_{roiw}[S_g/(1-S_{wr})]$ and $k_{roiw}(S_o/(1-S_{wr})]$.

The three-phase oil relative permeability is estimated using Aziz and Settari's version[13] of Stone's equation:

$$k_{ro} = k_{roiw}\left[\left(\frac{k_{row}}{k_{roiw}} + k_{rw}\right)\left(\frac{k_{rog}}{k_{roiw}} + k_{rg}\right) - \left(k_{rw} + k_{rg}\right)\right]. \quad \ldots\ldots\ldots\ldots\ldots\ldots (36)$$

The values of $\tilde{k}_{rg}$, $\tilde{k}_{rog}$, k_{rw}, and k_{row} are computed using either tabulated data or the following equations.

$$\tilde{k}_{rg} = k_{roiw}\left(\frac{S_g - S_{gr}}{1-S_{gr}-S_{wr}}\right)^{e_g}. \quad \ldots\ldots\ldots\ldots (37a)$$

$$\tilde{k}_{rog} = k_{roiw}\left(\frac{1-S_g-S_{org}-S_{wr}}{1-S_{org}-S_{wr}}\right)^{e_{og}}. \quad \ldots\ldots\ldots (37b)$$

$$k_{rw} = k_{rwro}\left(\frac{S_w - S_{wr}}{1-S_{wr}-S_{orw}}\right)^{e_w}. \quad \ldots\ldots\ldots\ldots (37c)$$

$$k_{row} = k_{roiw}\left(\frac{1-S_w-S_{orw}}{1-S_{wr}-S_{orw}}\right)^{e_{ow}}. \quad \ldots\ldots\ldots\ldots (37d)$$

The capillary pressure, P_{cog}, at the gas/oil interfacial tension, σ, is related to the capillary $\tilde{P}_{cog}$ (immiscible condition) by the following equation.

$$P_{cog} = \left(1-e^{-c\sigma}\right)\tilde{P}_{cog}, \quad \ldots\ldots\ldots\ldots\ldots\ldots (38)$$

where c is an adjustable positive number.

The gas/oil interfacial tension is calculated using the Macleod-Sugden correlation[14] and the viscosities of oil and gas are computed from a modified Jossi, Stiel, and Thodos correlation.[14]

The compositions y_{mo} and y_{mg}, which multiply T_o and T_g in Eq. 2, also can be evaluated at the upstream block. The use of this single-point upstream formulation for composition may cause excessive numerical dispersion. To reduce the numerical dispersion, a two-point upstream weighting for composition, similar to the development of Todd *et al.*[15] on relative permeabilities, is introduced.

Let i-1 and i-2 be the two upstream blocks of grid block i. The two-point upstream composition at the interface i-½ is obtained by extrapolating the composition in grid block i-1 and i-2 to that interface:

$$y_{m,i-\frac{1}{2}} = y_{m,i-1} + \frac{\Delta\ell_{i-1}}{\Delta\ell_{i-1} + \Delta\ell_{i-2}}\left(y_{m,i-1} - y_{m,i-2}\right), \quad \ldots\ldots\ldots\ldots\ldots\ldots\ldots\ldots (39)$$

where $\Delta\ell_{i-1}$ is the length of grid block i-1. To avoid overshoot and undershoot problems, the following constraints are introduced.

$$y_{m,i-\frac{1}{2}} \le \max\left(y_{m,i-1}, y_{m,i}\right) \quad \ldots\ldots\ldots\ldots\ldots (40a)$$

and

$$y_{m,i-\frac{1}{2}} \ge \min\left(y_{m,i-1}, y_{m,i}\right). \quad \ldots\ldots\ldots\ldots\ldots (40b)$$

Eqs. 39 and 40 apply to both oil and gas compositions. If only one hydrocarbon phase is present in grid block i-1, the global composition, z_m, is used instead of y_m in these equations.

Well Models

This section describes the formulation of rate- or pressure-constrained injection/production wells, and multiblock well completions. The rates are positive for injection wells and negative for production wells by conventions.

The molar flow rates for water and for component m into or from the ith grid block containing a well are

$$q_w = \rho_w^n Q_w^n \quad \ldots\ldots\ldots\ldots\ldots\ldots\ldots\ldots\ldots (41)$$

and

$$q_m = y_{mo}^n \rho_o^n Q_o^n + y_{mg}^n \rho_g^n Q_g^n, \quad \ldots\ldots\ldots\ldots\ldots (42)$$

where Q_j is the volumetric flow rate of phase $j(j = o,g,w)$.

For constant-rate injection wells, Q_j's are specified and the compositions and densities in Eqs. 41 and 42 are those of the injection fluid at $p_{o,i}^n$.

For constant-rate production wells, the compositions and densities are those of the ith grid block.

For constant-pressure injection wells, the volumetric flow rates (Q_j's) are determined from

$$Q_j = I_{wj}\left(p_{bh} - p_{o,i}^{n+1}\right), \; p_{bh} > p_{o,i}^{n+1}, \quad \ldots\ldots\ldots\ldots (43)$$

with

$$I_{wj} = \frac{2\pi khf\lambda_t}{\ln\left(C\frac{r_{eq}}{r_w}\right) + s}, \quad \ldots\ldots\ldots\ldots\ldots\ldots (44)$$

where C is a factor that takes into account the geometry of the grid block and the location of the well within it[16] and λ_t is the total mobility of the fluids in the grid block.[17]

For constant-pressure production wells, the flow rate of phase j is given by Eq. 43 with p_{bh} less than $p_{o,i}^{n+1}$ and λ_t in Eq. 44 is replaced by λ_j, the mobility of phase j in the grid block.

All the compositions and properties in Eqs. 41 through 44 are computed at time level n. Hence, it can be shown easily that $\partial q_w/\partial p_o^{n+1} = \partial q_h/\partial p_o^{n+1} = 0$ for constant rate wells and that

$$\frac{\partial q_w}{\partial p_o^{n+1}} = -I_{ww}\dot{\rho}_w \quad \ldots\ldots\ldots\ldots\ldots\ldots (45a)$$

and

$$\frac{\partial q_h}{\partial p_o^{n+1}} = -I_{wo}\rho_o - I_{wg}\rho_g \quad \ldots\ldots\ldots\ldots\ldots (45b)$$

for constant bottomhole pressure wells.

In many field-simulation problems, the well is completed through several grid blocks and the total rate of the multilayer well is specified. It is then necessary to determine the bottomhole pressure and the pressure along the portion of the well open to flow from the reservoir. The bottomhole pressure is the pressure that yields the specified flow rate. A schematic of a multiblock completion well is shown in Fig. 1 where, for conven-

TABLE 1—SATURATION PRESSURE AND SWELLING DATA

Component, mol%	Recombined Reservoir Fluid	Recombined Reservoir Fluid + CO_2			
CO_2	1.64	18.45	37.03	56.79	77.74
N_2	2.18	1.81	1.40	0.96	0.49
C_1	28.99	24.03	18.55	12.73	6.57
C_2	7.97	6.61	5.10	3.50	1.80
C_3	7.15	5.93	4.58	3.14	1.62
iC_4	1.21	1.00	0.77	0.53	0.27
nC_4	3.54	2.94	2.27	1.56	0.80
iC_5	2.00	1.66	1.28	0.88	0.45
nC_5	2.12	1.76	1.36	0.93	0.48
C_6^+	43.20	35.81	27.66	18.98	9.78
Properties					
C_6^+ density at 15.6 °C, g/mL	0.8358	0.8358	0.8358	0.8358	0.8358
C_6^+ molecular weight	178.47	178.47	178.47	178.47	178.47
Bubble-point pressure, psia (kPa)	2,300 (15 858)	2,705 (18 650)	2,945 (20 305)	3,515 (24 235)	6,000 (41 368)
Reservoir temperature, °F (°C)	206 (96.6)	206 (96.6)	206 (96.6)	206 (96.6)	206 (96.6)
Solution GOR*	746 (132.9)	1,079 (192.1)	1,336 (238.0)	2,662 (474.1)	5,836 (1039.4)
Swelling factor**	1.000	1.103	1.133	1.487	2.083
Calculated Data					
Bubble-point pressure, psia (kPa)	2,303 (15 880)	2,584 (17 814)	3,000 (20 681)	3,754 (25 884)	6,157 (42 449)
Solution GOR	665 (118.5)	966 (172.0)	1,489 (265.2)	2,567 (457.2)	5,903 (1051.3)
Swelling factor	1.000	1.084	1.227	1.503	2.170

*Cubic feet of gas at 14.7 psia and 60 °F per barrel of oil at 14.7 psia and 60 °F.
Cubic centimeters of gas at 1 atm and 15.6 °C per cubic centimeter of oil at 1 atm and 15.6 °C.
**Barrels of oil + CO_2 at saturation pressure and temperature per barrel of oil at saturation pressure and temperature.

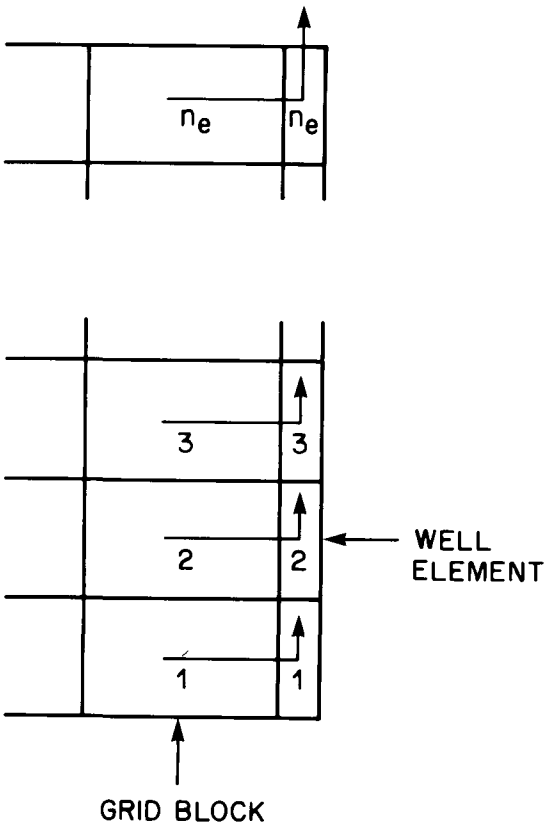

Fig. 1—Multiblock well completion.

TABLE 2—RECOMBINED RESERVOIR OIL COMPOSITION

Model Component	Actual Component	Composition (mol%)	
CO_2	CO_2	1.64	
N_2	N_2	2.18	
C_1	C_1	28.99	
C_2	C_2	7.97	
C_3	C_3	7.15	
nC_4	$iC_4 \pm nC_4$	4.75	
nC_5	$iC_5 \pm nC_5$	4.12	
C_6	C_6^+	19.40	43.20
C_{15}		11.90	
C_{22}		11.90	

Interaction Coefficients for C_6^+ Fractions			
C_6	0.105	0.120	0.090
C_{15}	0.120	0.120	0.110
C_{22}	0.150	0.120	0.145

ience, the grid block and corresponding well elements are numbered from one to n_e.

The volumetric flow rate of phase j into the ith well element is

$$Q_{j,i} = I_{wj,i}\left(p_{bh,i} - p_{o,i}^{n+1}\right)$$
$$\text{with } i = 1 \ldots n_e,\ j = o,g,w \quad \ldots\ldots\ldots (46)$$

and

$$p_{bh,i} = p_{bh,1} - H_i, \quad \ldots\ldots\ldots\ldots\ldots\ldots\ldots (47)$$

where H_i is the hydrostatic head of the fluid column at i with respect to Well Element 1:

$$H_1 = 0, \quad \ldots\ldots\ldots\ldots\ldots\ldots\ldots\ldots (48a)$$

$$H_i = \sum_{k=1}^{i-1} \tilde{\rho}_{t,k+\frac{1}{2}} g\left(D_{k-1} - D_k\right), \quad \ldots\ldots\ldots (48b)$$

and

$$\tilde{\rho}_{t,k+\frac{1}{2}} = \frac{\sum_j \left(\tilde{\rho}_j Q_j\right)_{k+\frac{1}{2}}}{\sum_j \left(Q_j\right)_{k+\frac{1}{2}}}, \text{ where } j = o,g,w.$$
$$\ldots\ldots\ldots\ldots\ldots\ldots\ldots\ldots\ldots (49)$$

In that treatment, frictional and kinetic energy effects are neglected in the wellbore. Assuming constant-pressure drawdown for all well elements—i.e.,

$$p_{bh,i}^{n+1} - p_{o,i}^{n+1} = p_{bh,k}^{n+1} - p_{o,k}^{n+1} \text{ where } k \neq i, \quad \ldots\ldots (50)$$

Eq. 49 yields

$$\tilde{\rho}_{t,k+\frac{1}{2}} = \frac{\sum_j \left(\tilde{\rho}_j I_{wj}\right)_{k+\frac{1}{2}}}{\sum_j \left(I_{wj}\right)_{k+\frac{1}{2}}}. \quad \ldots\ldots\ldots\ldots (51)$$

Let Q_t^* be the specified total flow rate. It can be shown that

$$p_{bh,1} = \frac{\sum_{i=1}^{n_e} \sum_j I_{wj,i}\left(p_{o,i}^{n+1} + H_i\right) + Q_t^*}{\sum_{i=1}^{n_e} \sum_j I_{wj,i}}.$$
$$\ldots\ldots\ldots\ldots\ldots\ldots\ldots\ldots\ldots (52)$$

The derivatives of the molar flow rates with respect to $p_{o,i}^{n+1}$ then are given by

$$\frac{\partial q_w}{\partial p_{o,i}^{n+1}} = I_{ww,i}\rho_{w,i}^n\left(\frac{\partial p_{bh,1}}{\partial p_{o,i}^{n+1}} - 1\right) \quad \ldots\ldots\ldots (53a)$$

and

$$\frac{\partial q_h}{\partial p_{o,i}^{n+1}} = \left(I_{wo,i}\rho_{o,i}^n + I_{wg,i}\rho_{g,i}^n\right)\left(\frac{\partial p_{bh,1}}{\partial p_{o,i}^{n+1}} - 1\right),$$
$$\ldots\ldots\ldots\ldots\ldots\ldots\ldots\ldots\ldots (53b)$$

where, from Eq. 52,

$$\frac{\partial p_{bh,i}}{\partial p_{o,i}^{n+1}} = \frac{\sum_j I_{wj,i}}{\sum_{i=1}^{n_e} \sum_j I_{wj,i}} \text{ with } j = o,g,w. \quad \ldots (54)$$

That above derivation involves rate constrained multiblock well completions. If the completion is pressure constrained—i.e., $p_{bh,1}$ is specified—the derivation is much simpler. The pressure in each well element can be obtained by using Eqs. 47 through 49 and the derivatives of the molar flow rates with respect to $p_{o,i}^{n+1}$ can be computed from Eq. 53 by setting $\partial p_{bh,1}/\partial p_{o,i}^{n+1}$ equal to zero.

From Eq. 54, $\partial p_{bh,1}/\partial_{o,i}^{n+1}$ is always less than one. Hence, $\partial q_w/\partial p_{o,i}^{n+1}$ and $\partial q_h/\partial p_{o,i}^{n+1}$ are always less than or equal to zero depending on the type of well. This guarantees that the Jacobian in Eq. 16 is always diagonally dominant.

Examples

A few applications of the model that include one- and two-dimensional examples of CO_2 displacements are described in this section. The CO_2/reservoir oil system of Sigmund *et al.*[18] is used with a different representation for the C_6^+ fraction, which yields a better match of the phase-behavior data. Composition and physical properties of the recombined reservoir fluid with CO_2 are given in Table 1. The phase behavior is predicted using the Peng-Robinson equation of state with components shown in Table 2.

Slim-Tube Displacement

In this example, the effect of interfacial tension on simulation results is examined. The slim-tube tests were conducted in a 0.375-in.-OD × 0.305-in.-ID stainless steel tube, 58.79 ft long, packed with 140-mesh beads that had a liquid permeability of about 5.07 darcy. The pore volume of the tube was about 21.85 cu in., which corresponds to a porosity of 42.4%. The injection rate was 0.976 cu in/hr.

The following relative permeability curves were used in the simulation.

$$\tilde{k}_{rg} = S_g^{\,2},$$

$$\tilde{k}_{ro} = \left(\frac{S_o - 0.2}{0.8}\right)^{2.5},$$

$$k_{rg} = \left(1 - e^{-\sigma/3.31}\right)\tilde{k}_{rg} + e^{-\sigma/3.31} S_g,$$

$$k_{ro} = \left(1 - e^{-\sigma/3.31}\right)\tilde{k}_{ro} + e^{-\sigma/3.31} S_o,$$

where σ is in dyne/cm. The value of 3.31 corresponds to the interfacial tension in dyne/cm between the vapor and liquid phases obtained by flashing the recombined reservoir oil at 1,885.5 psia and 205.9 °F. The capillary pressure is assumed negligible. The slim tube was represented by a 25 grid-block system.

Figs. 2a and 2b show the experimental and computed oil recovery (calculated from the standard volume of original oil in place) at two different pressures, 3,000 and 3,840 psia and a temperature of 205.9 °F. Results obtained with fixed relative permeability curves that are independent of interfacial tension (i.e., $k_{ro} = \tilde{k}_{ro}$, $k_{rg} = \tilde{k}_{rg}$) are shown also.

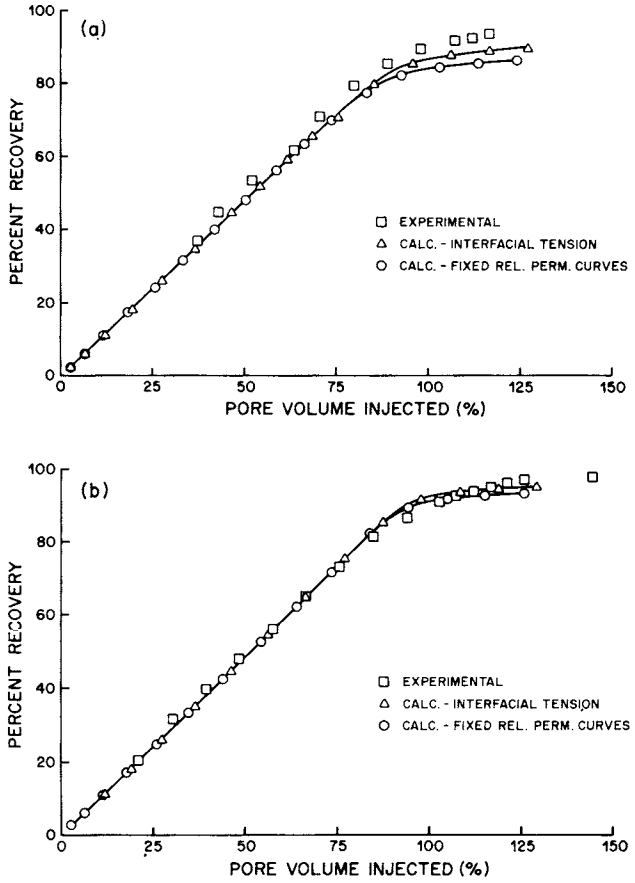

Fig. 2—Oil recovery curve at (a) 20 684 kPa and (b) 23 993 kPa.

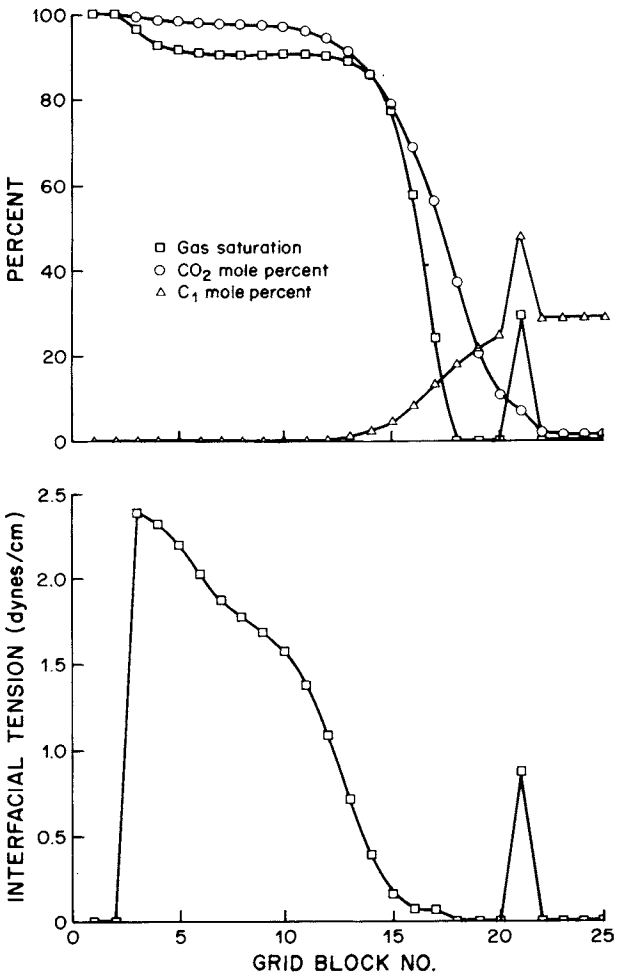

Fig. 3—Saturation, composition, and interfacial tension profiles at 20 684 kPa and 61.9% PV injected.

TABLE 3—DATA FOR AREAL RUN

Dimensions, ft (m)	
Length	2,639 (804.3)
Width	2,639 (804.3)
Thickness	15 (4.6)
Permeability, darcy	0.030
Porosity, fraction	0.020
Rock compressibility, kPa^{-1}	0
Initial reservoir pressure, psia (kPa)	2,466 (17 000)
Temperature, °F (°C)	206 (96.6)
Initial water saturation, fraction	0.4
Relative permeability data (Eq. 37)	
$k_{roiw} = k_{rwro}$	1.0
S_{org}	0.3
S_{gr}	0.0
S_{orw}	0.1
S_{wr}	0.2
e_{og}	2.0
$e_g = e_{ow}$	1.5
e_w	2.5

TABLE 4—DATA FOR CROSS-SECTIONAL RUN

Dimensions, ft (m)	
Length	6,597 (2010.860)
Width	330 (100.543)
Thickness	60 (18.288)
Rock compressibility, kPa^{-1}	0
Initial average reservoir pressure, psia (kPa)	2,466 (17 000)
Temperature, °F (°C)	206 (96.6)
Initial water saturation, %	0
Relative permeability data	
$k_{roiw} = k_{rwro}$	1.0
S_{org}	0.2
$S_{gr} = S_{orw} = S_{wr}$	0.0
e_{og}	2.0
e_g	1.5
$e_{ow} = e_w$	1.0

Layer	Permeability (darcy) k_H	Permeability (darcy) k_v	Porosity (fraction)
1 (bottom)	0.020	0.002	0.17
2	0.040	0.004	0.25
3	0.030	0.003	0.20
4	0.010	0.001	0.15

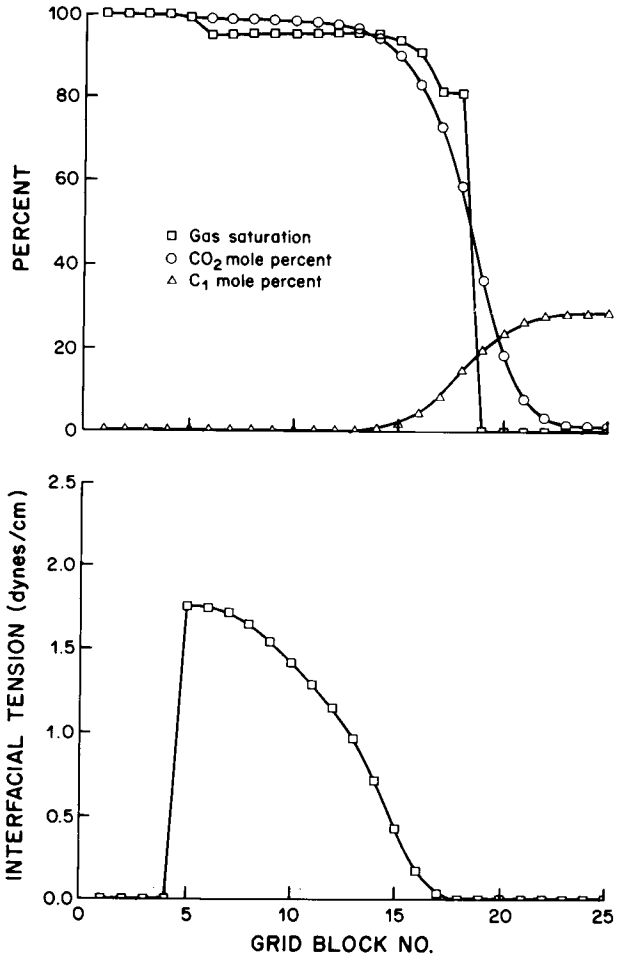

Fig. 4—Saturation, composition, and interfacial tension profiles at 23 993 kPa and 66.7% PV injected.

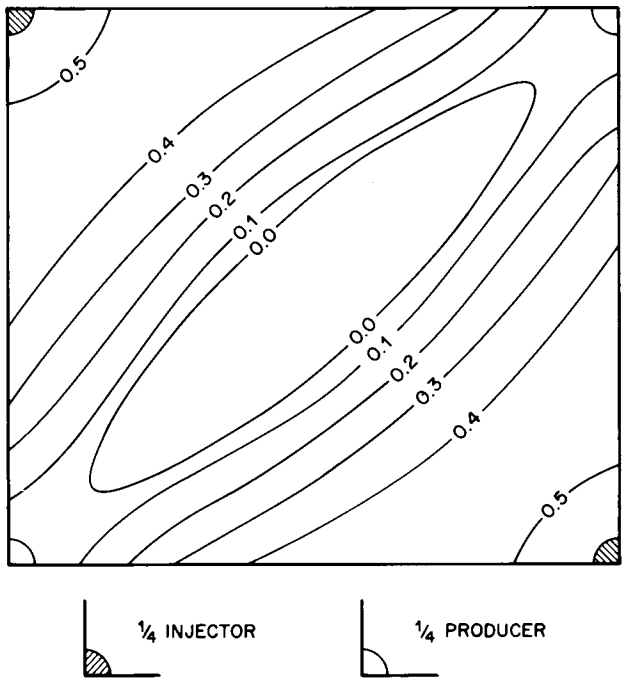

Fig. 5—Gas saturation contours at 3,582 days.

Higher recovery is obtained when interfacial tension is considered. At 1.29 PV injected, the additional recoveries are 3.46 and 1.59% at 3,000 and 3,480 psia, respectively. Fig. 3 shows the computed profiles of CO_2 and C_1 concentration, gas saturation, and interfacial tension at 3,000 psia and 61.9% PV injected. One also can observe a leading methane bank (grid block 21), followed by a miscible region (grid blocks 18 through 20). It is interesting to note that the interfacial tension decreases sharply as the miscible region is approached and becomes almost zero just behind the miscible region (grid blocks 16 and 17). Fig. 4 shows the computed profiles for the same variables at 3,480 psia and 66.7% PV injected; note a shorter transition zone (the gas saturation decreases more abruptly) and the absence of a leading C_1 bank.

The influence of interfacial tension on the recovery depends on the size of the region of very low interfacial tension[19] (less than 10^{-1} dyne/cm). That region is larger in the displacement at 3,000 psia, which is a multiple-contact miscible process, than the one at 3,480 psia, which is close to a first contact miscible process. This explains why the computed additional recovery due to interfacial tension effects is higher for the former displacement (3.46% compared with 1.59% at 1.29 PV injected). However, these effects are quite small and fixed relative permeability curves could have been used for this example. These fixed curves should be thought of as average curves that account for the effects of porous medium heterogeneities and changes in interfacial tension and mobility ratios with respect to pressure and composition.

The program took five iterations per time step and the average computation time on the Honeywell DPS 2 with Multics operating system is 0.471 seconds per time step per grid block. Direct elimination was used to solve the pressure equation. About 50 time steps were required to inject 1.36 PV of CO_2.

CO_2 Areal Displacement

Half of a 5-spot pattern of a CO_2 injection process was simulated using an 8×8 areal grid system that covers an area of 160 acres. Pertinent data for the simulation are given in Table 3. The bottomhole pressures for injectors and producers are 3,000 and 2320.6 psia, respectively. The interfacial tension and capillary effects are assumed negligible. Fig. 5 shows the gas saturation contour at 3,582 days. Simulation results show an enrichment zone where the densities of oil and gas gradually approach each other. However, no miscible bank was formed and the process was immiscible.

The program took 6.5 iterations per time step and the average execution time on the Honeywell DPS 2 was 0.757 seconds per time step per grid block when direct

TABLE 5—PROGRAM PERFORMANCE FOR SOME TYPICAL AREAL RUNS WITH THREE COMPONENTS

	Grid System			
	10 × 10	13 × 13	17 × 17	25 × 25
Average execution time per grid block per time step, CPU seconds*				
Direct elimination	0.125 (0.022)	0.112 (0.020)	0.121 (0.022)	0.153 (0.027)
ICCG (0)	0.134 (0.024)	0.122 (0.022)	0.115 (0.021)	0.119 (0.021)
Average number of iterations per time step	6.2	5.8	6.2	6.2
Average number of iterations in ICCG (0) routine	12.2	15.1	18.4	25.4

*Execution times are for the Honeywell DPS 2 with Multics operating system. Figures in parentheses represent the equivalent execution time for the CDC 6600 based on our benchmark runs.

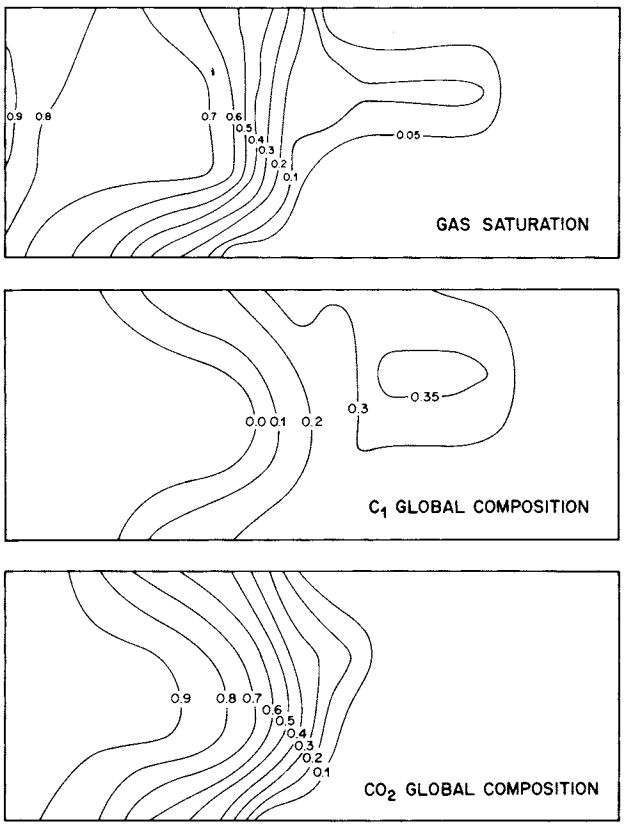

Fig. 6—Gas saturation and composition contours at 3,778 days.

elimination was used to solve the pressure equation. Fifty-four time steps were required to inject 89.9% PV of CO_2. The execution time when the ICCG(0) was used was 1.03 times higher and about 12 iterations were needed in the conjugate gradient routine to obtain the solution of the pressure equation. This shows that for a bandwidth of 17, direct elimination is still faster than ICCG(0).

Cross-Sectional Displacement

Cross-sectional runs were performed for CO_2 injection into a stratified reservoir. A 20 × 4 grid system is used to represent the reservoir. Pertinent data for this study are given in Table 4. CO_2 was injected at a pressure of 3,000 psia. During the first 45 days, the oil was produced at a constant rate of 251.6 RB/D. After that, a bottomhole pressure of 2,290.6 psia was maintained in the producing multiblock completion well. The capillary pressure and interfacial tension are assumed negligible.

Fig. 6 shows the gas saturation and CO_2 and C_1 global mole fractions contours at 3,778 days (33.65% PV injected). One can observe a leading methane-rich gas bank in the third and fourth layers. The simulation results show the formation of a near miscible region following the methane bank. Gas breaks through after 6,588 days (66.8% PV injected), and the recovery at 8,692 days (1.04 PV injected) is 71.8%.

Direct elimination was used to solve the pressure equation. The program took six iterations per time step, and the average execution time on the Honeywell DPS 2 was 0.658 seconds per time step per grid block. Ninety-nine time steps were required to inject 1.04 PV of CO_2.

Computational Experience

The computation times reported earlier are for the Honeywell DPS 2 with Multics operating system. On the basis of some benchmark runs, the execution time for the Honeywell DPS 2 is five and six-tenths times that of CDC 6600.

To compare the computing time requirements of our model with the ones of Fussell and Fussell[7] and Coats,[9] a series of areal runs was made using the ternary system C_1-nC_4-nC_{10}. The execution times for both direct elimination and ICCG(0) along with other pertinent information are reported in Table 5. The numbers show that the execution time is of the same order as the model of Fussell and Fussell. The use of iterative conjugate gradient method takes more time than direct elimination for an areal system with a bandwidth less than 35.

Conclusions

This paper presents an implicit-pressure explicit-composition and explicit-saturation method for the simulation of multidimensional compositional problems. Although the convergence near the solution is not quadratic as in the model by Fussell and Fussell,[7] it is simple to program and its performance is very satisfactory.

Most of the important mechanisms of high-pressure gas, enriched-gas, and CO_2 floods have been taken into account. The iterative scheme can be modified to include the solubility of some components such as CO_2, SO_2, and H_2S into the water phase using Henry's law.

One desirable feature of the formulation is the symmetric and diagonally dominant pressure matrix that allows the use of ICCG(0) methods for large problems. The use of the ICCG(0) method yields better execution time than direct elimination for bandwidths greater than 35. A two-point upstream formulation for composition reduces the numerical dispersion and an efficient flash-calculation method permits the use of the model around the critical point. The drawback of the formulation is the time-step size limitation due to the explicit treatment of compositions and transmissibilities.

The model has been tested against slim-tube experimental data, and satisfactory results were obtained. Areal and cross-sectional runs for hypothetical field problems yield physically reasonable results with all the typical enrichment phenomena in the transition zone and the gravity segregation effects.

Nomenclature

A = area perpendicular to flow
c_f = rock compressibility
c_w = water compressibility
C = shape factor in well model
D = depth (measured positive down)
e = exponential function
f = well fraction
f_{mj} = fugacity of component m in phase j ($j = o,g$)
g = gravity acceleration
h = thickness
H = head in multiblock well completion model
$I_{w,j}$ = well index for phase j ($j = o,g,w$)
J = Jacobian matrix
k = permeability
k_{rj} = relative permeability to phase j ($j = o,g,w$)
k_{roiw} = relative permeability to oil or to gas at irreducible water saturation
k_{rog} = relative permeability to oil in gas/liquid system at irreducible water saturation
k_{row} = relative permeability to oil in oil/water system
k_{rwro} = relative permeability to water at residual oil saturation
k_H = horizontal permeability
k_v = vertical permeability
L = mole fraction of liquid phase in hydrocarbon system
n_e = number of well elements in a multiblock well completion
n_b = number of grid blocks
p_j = pressure of phase j ($j = o,g,w$)
P_{cog} = oil/gas capillary pressure
P_{cwo} = water/oil capillary pressure
q_h = molar injection/production rate of hydrocarbon
q_m = molar injection/production rate of component m
q_w = molar injection/production rate of water
Q_j = volumetric injection/production rate of phase j ($j = o,g,w$)
r_{eq} = equivalent radius in well model
r_w = well radius
R = universal gas constant
s = skin factor
S_j = saturation of phase j ($j = o,g,w$)
S_{jr} = residual saturation of phase j
S_{org} = residual oil saturation in gas/liquid system at irreducible water saturation
S_{orw} = residual oil saturation in water/oil system
t = time
T = temperature
T_j = transmissibility of phase j ($j = o,g,w$)
V = mole fraction of vapor phase in hydrocarbon system
V_b = block volume
y_{mj} = mole fraction of component m in phase j ($j = o,g$)
z_m = global mole fraction of component m in hydrocarbon system
Z = compressibility factor
$\alpha = \theta\rho_w S_w + \rho_o S_o + \rho_g S_g$
$\gamma = g\tilde{\rho}_j$, gradient of phase j
Δ = difference operator
$\theta = (\rho_o S_o + \rho_g S_g)/[\rho_w (S_o + S_g)]$
$\lambda_j = k_{rj}/\mu j$, mobility of phase j
$\lambda_t = \sum_j \lambda_j$, total mobility
μ_j = viscosity of phase j
ν = number of hydrocarbon components
ρ_j = molar density of phase j
$\tilde{\rho}_j$ = mass density of phase j
σ = interfacial tension
ϕ = porosity
Φ_j = potential of phase j ($j = o,g,w$)

Superscripts

(ℓ) = iteration level
n = old time level
$n+1$ = new time level

Subscripts

bh = bottomhole
c = critical
g = gas
i,k = grid block indices
j = phase index
m = component index
o = oil
t = total
w = water
x,y,z = coordinate directions

Difference Notation

$$\Delta T \Delta p = \Delta_x T_x \Delta p_x + \Delta_y T_y \Delta p_y + \Delta_z T_z \Delta p_z$$

and

$$\Delta_x T_x \Delta p_x = T_{x,i+\frac{1}{2}}\left(p_{i+1} - p_i\right) - T_{x,i-\frac{1}{2}}\left(p_i - p_{i-1}\right),$$

where $T_{x,i+\frac{1}{2}}$ is the x direction transmissibility between grid block i and $i+1$.

Acknowledgments

This research is supported by the Alberta/Canada Energy Resources Research Fund administered by the Dept. of Energy and Natural Resources of the Province of Alberta. We thank P.K.W. Vinsome for his helpful comments and suggestions on this work and A. Behie for programming the conjugate gradient routine. The phase-behavior package used in the simulator is a modified version of the Hyprotech fluid properties program (HYPROP).

References

1. Zudkevitch, D. and Joffe, J.: "Correlation and Prediction of Vapor-Liquid Equilibrium with the Redlich-Kwong Equation of State," *AIChE J.* (Jan. 1970) **16**, 112-119.
2. Soave, G.: "Equilibrium Constants from a Modified Redlich-Kwong Equation of State," *Chem. Eng. Sci.* (1977) **27**, 1197-1203.
3. Peng, D.Y. and Robinson, D.B.: "A New Two-Constant Equation of State," *Ind. Eng. Chem. Fund.* (1976) **15**, 59-64.
4. Bishnoi, P.R., Heidemann, R.A., and Shah, M.K.: "Calculation of Thermodynamic Properties of Bitumen Systems," paper presented at the CIM Canada-Venezuela Oil Sands Symposium, Edmonton, Alta., May 30-June 4, 1977.
5. Yarborough, L.: "Application of a Generalized Equation of State to Petroleum Reservoir Fluids," paper presented at the I&EC Symposium on Equations of State in Engineering and Research, 176th ACS Natl. Meeting, Miami Beach, FL, Sept. 10-15, 1978.
6. Katz, D.L. and Firoozabadi, A.: "Predicting Phase Behavior of Condensate/Crude-Oil Systems Using Methane Interaction Coefficients," *J. Pet. Tech.* (Nov. 1978) **30**, 1649-1655.
7. Fussell, L.T. and Fussell, D.D.: "An Iterative Technique for Compositional Reservoir Models," *Soc. Pet. Eng. J.* (Aug. 1979) **19**, 211-220.
8. Fussell, D.D. and Yanosik, J.L.: "An Iterative Sequence for Phase Equilibrium Calculations Incorporating the Redlich-Kwong Equation of State," *Soc. Pet. Eng. J.* (June 1978)**18**, 173-182.
9. Coats, K.H.: "An Equation of State Compositional Model," *Soc. Pet. Eng. J.* (Oct. 1980) 363-376.
10. Kazemi, H., Vestal, C.R., and Shank, G.D.: "An Efficient Multicomponent Numerical Simulator," *Soc. Pet. Eng. J.* (Oct. 1978) **18**, 355-368.
11. Nghiem, L.X. and Aziz, K.: "A Robust Iterative Method for Flash Calculations Using the Soave-Redlich-Kwong or the Peng-Robinson Equation of State," paper SPE 8285 presented at the SPE 54th Annual Meeting, Las Vegas, Sept. 23-26, 1979.
12. Meijerink, J.A. and van der Vorst, H.A.: "An Iterative Solution Method for Linear Systems of which the Coefficient Matrix is a Symmetric M-Matrix," *Math. Comp.* (Jan. 1977) **31**, 148-162.
13. Aziz, K. and Settari, A.: *Petroleum Reservoir Simulation*, Applied Science Publishers, London (1979) 36.
14. Reid, R.C., Prautsnitz, J.M., and Sherwood, T.K.: *The Properties of Gases and Liquids*, third edition, McGraw-Hill Inc., New York City (1977) 426, 614.
15. Todd, M.R., O'Dell, P.M., and Hirasaki, G.J.: "Methods for Increased Accuracy in Numerical Reservoir Simulators," *Soc. Pet. Eng. J.* (Dec. 1972) **12**, 515-530.
16. Au, A.D.K., Behie, A., Rubin, B., and Vinsome, P.K.W.: "Techniques for Fully Implicit Reservoir Simulation," paper SPE 9302 presented at the SPE 55th Annual Meeting, Dallas, Sept. 21-24, 1980.
17. Chappelear, J.E. and Williamson, A.S.: "Representing Wells in Numerical Reservoir Simulation—Theory and Implementation," paper SPE 7697 presented at the SPE Fifth Symposium on Reservoir Simulation, Denver, Feb. 1-2, 1979.
18. Sigmund, P.M., Aziz, K., Lee, J.T., Nghiem, L.X., and Mehra, R.: "Laboratory CO_2 Floods and Their Computer Simulation," paper presented at the 10th World Pet. Cong., Bucharest, Sept. 1979.
19. Bardon, C. and Longeron, D.G.: "Influence of Very Low Interfacial Tensions on Relative Permeability," *Soc. Pet. Eng. J.* (Oct. 1980) **20**, 391-401.

SI Metric Conversion Factors

acre	×	4.046 873 E + 03	=	m^2
atm	×	1.013 250* E + 02	=	kPa
bbl	×	1.589 873 E - 01	=	m^3
cu in.	×	1.638 706 E + 01	=	cm^3
cu ft	×	2.831 685 E - 02	=	m^3
dyne	×	1.0* E - 02	=	mN
g mol	×	1.0* E - 03	=	kmol
°F		(°F - 32)/1.8	=	°C
psia	×	6.894 757 E + 00	=	kPa

*Conversion factor is exact.

SPEJ

Original manuscript received in Society of Petroleum Engineers office July 21, 1980. Paper accepted for publication April 21, 1981. Revised manuscript received Sept. 23, 1981. Paper (SPE 9306) first presented at the SPE 55th Annual Technical Conference and Exhibition held in Dallas Sept. 21-24, 1980.

Discussion of Compositional Modeling With an Equation of State

SPE 10894

Jahan Mansoori, SPE, Phillips Petroleum Co.

The following addresses "Compositional Modeling With an Equation of State," L.X. Nghiem, D.K. Fong, and K. Aziz (Dec. 1981 *SPEJ*, Pages 687–698).

The compositional formulation as presented calls for the solution of the pressure equation given by

$$\Delta\Big[\theta T_w{}^n(\Delta P_o{}^{n+1}-\Delta P_{cwo}{}^n-\gamma_w{}^n\Delta h)+T_o{}^n(\Delta P_o{}^{n+1}-\gamma_o{}^n\Delta h)+T_g{}^n(\Delta P_o{}^{n+1}+\Delta P^n_{cog}-\gamma_g{}^n\Delta h)+\eta^n\Big]+\theta q_w+q_{Hc}-\frac{V_b}{\Delta t}\left(\phi^{n+1}\alpha^{n+1}-\phi^n\alpha^n\right)=0. \quad \ldots\ldots\ldots\ldots (1)$$

The Newton method adopted for the solution requires an approximation to the term $\partial(\phi\alpha)/\partial P_o$ where ϕ is the grid-block porosity and α is defined as

$$\alpha=\theta\xi_w S_w+\xi_o S_o+\xi_g S_g. \quad \ldots\ldots\ldots\ldots\ldots\ldots (2)$$

The following approximation to $\partial\alpha/\partial P_o$ is presented by the authors, in which the terms $\partial S_w/\partial P_o$, $\partial S_o/\partial P_o$, $\partial S_g/\partial P_o$, $\partial Y_{mo}/\partial P_o$, and $\partial Y_{mg}/\partial P_o$ are neglected because of their complicated computation:

$$\frac{\partial\alpha}{\partial P_o}=\theta S_w\frac{\partial\xi_w}{\partial P_o}+S_o\frac{\partial\xi_o}{\partial P_o}+S_g\frac{\partial\xi_g}{\partial P_o}. \quad \ldots\ldots (3)$$

Although this equation leads to a diagonally dominant Jacobian matrix using SRK or PR equation of state, experience has shown that under certain reservoir flow conditions where the time variations of hydrocarbon phase saturations are considerably more pronounced than the respective changes in their physical properties, Eq. 3 is not valid and the Newton method may lead to a diverging, or oscillatory, or slow-converging system of equations. A new formulation has been presented to overcome this difficulty.

A situation where an unstable behavior first was observed was during the simulation of pressure decline of an undersaturated reservoir in which a hydrocarbon gas phase was generated as the reservoir pressure passed through the bubble point. Since variation in water saturation is negligible compared with that of hydrocarbon phases, Eq. 2 can be differentiated with respect to pressure to give

$$\frac{\partial\alpha}{\partial P_o}=\theta S_w\frac{\partial\xi_w}{\partial P_o}+\frac{\partial}{\partial P_o}(\xi_o S_o+\xi_g S_g), \quad \ldots\ldots (4)$$

where the term in parentheses represents the total hydrocarbon mass in a grid block. From a material balance on oil and gas phases, the vapor phase fraction can be derived as

$$V=\frac{\xi_g S_g}{\xi_o S_o+\xi_g S_g}. \quad \ldots\ldots\ldots\ldots\ldots\ldots (5)$$

Using the phase saturation constraint

$$S_o+S_g+S_w=1,$$

Eq. 5 yields

$$S_g=\frac{V\xi_o(1-S_w)}{\xi_g+V(\xi_o-\xi_g)}.$$

The total hydrocarbon mass in each grid block, therefore, can be derived from Eq. 5 as

0197-7520/82/0041-0894$00.25

$$\xi_o S_o + \xi_g S_g = \frac{\xi_g}{V} \frac{V\xi_o(1-S_w)}{\xi_g + V(\xi_o - \xi_g)}$$
$$= \frac{\xi_o \xi_g (1-S_w)}{\xi_g + V(\xi_o - \xi_g)}. \quad \ldots\ldots\ldots\ldots (6)$$

Since S_w is treated as a constant, Eq. 6 is differentiated to give

$$\frac{\partial}{\partial P_o}(\xi_o S_o + \xi_g S_g) = (1-S_w)\frac{\partial}{\partial P_o}\left[\frac{\xi_g \xi_o}{\xi_g + V(\xi_o - \xi_g)}\right]$$
$$\ldots\ldots\ldots\ldots (7)$$

or

$$\frac{\partial}{\partial P_o}(\xi_o S_o + \xi_g S_g)$$
$$= \frac{\xi_o' \xi_g^2 + V(\xi_o^2 \xi_g' - \xi_g^2 \xi_o') - V'\xi_o \xi_g (\xi_o - \xi_g)}{[\xi_g + V(\xi_o - \xi_g)]^2}$$
$$\cdot (1-S_w), \quad \ldots\ldots\ldots\ldots (8)$$

where primes indicate the derivative with respect to pressure.

This equation also provides the correct values for the two limiting cases of $S_o = 0$ (only gas phase present) or $S_g = 0$ (only oil phase present) using $V = V' = 0$ for the former and $V = 1$, $V' = 0$ for the latter. To study the effect of this approximation on the diagonal dominance of the Jacobian matrix, it can be shown easily that, under the conditions of

$$\xi_o > \xi_g > 0 \quad \ldots\ldots\ldots\ldots (9)$$

$$\xi_g' > \xi_o' > 0 \quad \ldots\ldots\ldots\ldots (10)$$

$$V' < 0, \quad \ldots\ldots\ldots\ldots (11)$$

Eq. 8 yields a positive value that contributes to the stability of Newton's method. Some or all of these conditions may not be satisfied for retrograde condensation process. The implications of this situation have yet to be explored. For computational purposes, V' in Eq. 8 may be approximated by

$$V' = \frac{V_{|\tilde{z},\tilde{P}} - V_{|\tilde{z},\tilde{P}-\Delta P}}{\Delta P},$$

where $\tilde{z}$ and $\tilde{P}$ are the latest calculated values of overall composition and pressure, respectively, for each grid block and ΔP is a reasonably selected pressure increment. The phase behavior subroutine is called each time to calculate V' during the simulation. Fig. 1 presents the residual-of-pressure equation, which is a measure of convergence vs. the number of iterations for the two methods of approximations. The method presented here reached the convergence criteria within about six iterations, while the other technique indicated an oscillatory behavior.

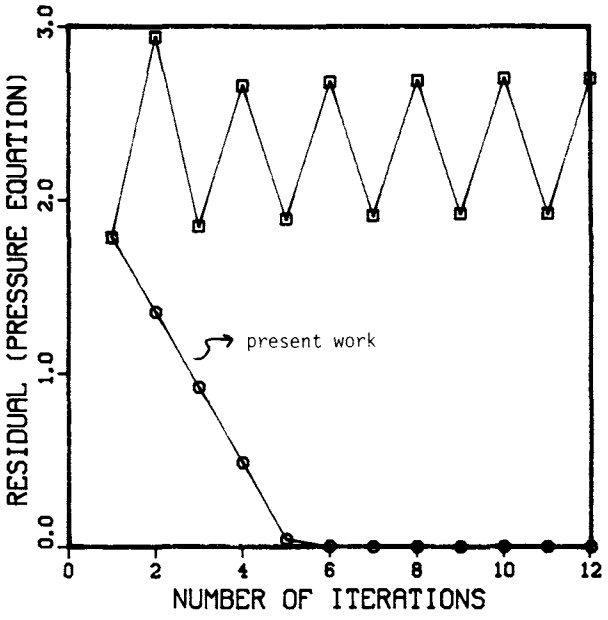

Fig. 1—Numerical behavior of Newton method for the two approximations of $\partial(\phi\alpha)/\partial P_o$.

Nomenclature

h = depth (measured positive down)
P_o = oil phase pressure
P_{cog} = oil-gas capillary pressure
P_{cwo} = water-oil capillary pressure
q_{HC} = molar injection/production rate of hydrocarbon
q_w = molar injection/production rate of water
S_j = saturation of phase j ($j=o,g,w$)
t = time
T_j = transmissibility of phase j ($j=o,g,w$)
V = mole fraction of vapor phase in hydrocarbon system
V_b = block volume
Y_{mg} = mole fraction of component m in phase j ($j=o,g$)
Z_m = overall mole fraction of component m
$\alpha = \theta\xi_w S_w + \xi_g S_g + \xi_o S_o$
η = contribution of dispersion effect
$\theta = (\xi_o S_o + \xi_g S_g)/[\xi_w(S_o + S_g)]$
ξ_j = molar density of phase j
ϕ = porosity
Δ = difference operator

SPEJ

Author's Reply to Discussion of Compositional Modeling With an Equation of State

SPE 10903

Long X. Nghiem, SPE, Computer Modelling Group

We have observed the same convergence problems described by Mansoori with certain fluids under certain reservoir flow conditions. They usually occur during pressure decline across the bubble point of an oil reservoir or the dewpoint of a gas condensate reservoir.

Under certain circumstances, during the iteration of the pressure equation, the gas released from an oil while pressure declines below the bubble point affects the approximate Jacobian described in our paper in such a way that the pressure increases after the subsequent iteration, and all or most of the gas goes back into solution. This creates a vicious circle and yields oscillations. The same reasoning applies to certain gas condensate reservoirs as the pressure declines below the dewpoint.

A solution to this problem is to use a damping factor in the update of the pressure solution—i.e.,

$$p_{o,k}^{(\ell+1)} = p_{o,k}^{(\ell)} + \omega^{(\ell)} \delta p_k{}^{(\ell)}, \quad k=1 \ldots n_b, \quad \ldots\ldots (1)$$

where $\delta p_k^{(\ell)}$ is the change in pressure obtained by solving our Eq. 15, and $\omega^{(\ell)}$ is a damping factor $(0<\omega^{(\ell)} \leq 1)$ that allows a smooth convergence to the solution. Note that ω can vary with the iteration level (ℓ). An appropriate selection of $\omega^{(\ell)}$ will prevent oscillations.

Mansoori's Discussion provides another method to improve the convergence of the algorithm described in our paper by including $\partial V/\partial p_o$ in the derivative $\partial\alpha/\partial p_o$. This method requires one additional flash calculation per grid block per iteration to compute $\partial V/\partial p_o$. Since no data were provided, we were unable to compare Mansoori's approach with ours.

Coats[1] has reported anomalous pressure response even for fully implicit simulators.

Nomenclature

n_b = number of grid blocks
$p_{o,k}$ = oil pressure of kth grid block
V = vapor mole fraction
α = defined in Eq. 13 of our paper
δp_k = change in pressure
ω = damping factor
(ℓ) = iteration level

Reference

1. Coats, K.H.: "Reservoir Simulation: A General Model Formulation and Associated Physical/Numerical Sources of Instability," *Boundary and Interior Layers—Computational and Asymptotic Methods*, J.J.H. Miller (ed.), Boole Press, Dublin (1980).

0197-7520/82/0041-0903$00.25

Errata

"Author's Reply to Discussion of Compositional Modeling With an Equation of State," April *SPEJ*, Page 204, listed only one author. Khalid Aziz, Computer Modelling Group, coauthored the Reply. The editors regret this omission and thank the other author, Long Nghiem, for pointing it out.

Also in the April issue, an error is noted by author Johan Mansoori in his "Discussion of Compositional Modeling With an Equation of State." The last equation (unnumbered) in Col. 1, Page 203, should read

$$V' = \frac{V_{|\bar{z},\bar{P}} - V_{|\bar{z},\bar{P}-\Delta P}}{\Delta P},$$

The editors regret these errors and thank the authors for pointing them out.